

Computing X-Ray Absorption Spectra from Linear-Response Particles atop Optimized Holes

Diptarka Hait,^{*,†,‡} Katherine J. Oosterbaan,[†] Kevin Carter-Fenk,[†] and Martin Head-Gordon^{*,†,‡}

[†]*Kenneth S. Pitzer Center for Theoretical Chemistry, Department of Chemistry, University of California, Berkeley, California 94720, USA*

[‡]*Chemical Sciences Division, Lawrence Berkeley National Laboratory, Berkeley, California 94720, USA*

E-mail: diptarka@berkeley.edu; mhg@cchem.berkeley.edu

Abstract

State specific orbital optimized density functional theory (OO-DFT) methods like restricted open-shell Kohn-Sham (ROKS) can attain semiquantitative accuracy for predicting X-ray absorption spectra of closed-shell molecules. OO-DFT methods however require that each state be individually optimized. In this work, we present an approach to generate an approximate core-excited state density for use with the ROKS energy ansatz, that is capable of giving reasonable accuracy without requiring state-specific optimization. This is achieved by fully optimizing the core-hole through the core-ionized state, followed by use of electron-addition configuration interaction singles (EA-CIS) to obtain the particle level. This hybrid approach can be viewed as a DFT generalization of the static-exchange (STEX) method, and can attain ~ 0.6 eV RMS error for the K-edges of C-F through the use of local functionals like PBE and OLYP. This ROKS(STEX) approach can also be used to identify important transitions for full

OO ROKS treatment, and can thus help reduce the computational cost for obtaining OO-DFT quality spectra. ROKS(STEX) therefore appears to be a useful technique for efficient prediction of X-ray absorption spectra.

Linear-response time dependent density functional theory^{1,2} (LR-TDDFT, henceforth simply referred to as TDDFT) is currently the most popular method for modeling electronic excited states. The popularity of TDDFT is a consequence of several factors, with perhaps the most important ones being computational efficiency and ability to simultaneously calculate multiple states. These two factors permit TDDFT to appear near ‘black-box’ to casual users, as the lowest n roots for a given system can be usually obtained by requesting software packages to compute N roots (where N is larger than n by a factor of 2-5), for relatively low computational cost and without any prior knowledge about the nature of the states. TDDFT is also formally exact,³ although this is of little practical relevance as the required exact time-dependent exchange-correlation (xc) kernel is unknown and approximate time-independent (ground state) density functionals have to be usually employed.² A particularly difficult challenge for TDDFT is that the LR protocol magnifies ground state delocalization errors^{4,5} to catastrophic proportions in the excited state. This has been widely recognized and studied for long-range charge-transfer (CT) states,^{2,6,7} with the TDDFT excitation energies being extremely sensitive to the proportion of Hartree-Fock (HF) exchange employed in the xc functional. TDDFT using time-independent kernels (the so-called adiabatic local density approximation or ALDA²) is also incapable of describing double excitations,⁸ leading to poor performance for open-shell systems^{9,10} and in describing bond dissociation.¹¹

Core-level excitations are another well-known regime of TDDFT failure, as the LR protocol is unable to fully describe the effect of forming a core-hole. Excitation energy errors of ~ 10 eV (vs experimental X-ray absorption spectra) are typical for second period elements like C,N,O and F, ranging from systematic underestimation with pure density functionals like BLYP¹² to systematic overestimation for pure HF.¹³ Even larger errors are observed for heavier elements. It is however worth noting that some highly specialized functionals have

been developed for predicting X-ray absorption energies,¹⁴ although the overall quality of the predicted spectra often leaves room for improvement.^{10,15} Much progress has also been made on wavefunction-based approaches for simulating core spectroscopy¹⁶⁻¹⁹ as the popularity of experimental core spectroscopy grows due to its value as a sensitive site-specific and time-resolved reporter on chemical dynamics.^{20,21}

State-specific orbital optimized (OO) methods¹⁵ offer a more robust route for addressing many of the shortcomings of TDDFT, as they permit relaxation of the excited state density beyond linear response. In particular, they have been quite effective at predicting core-level spectra of second period elements, with the Δ SCF method²² attaining ~ 0.5 eV errors for singlet K-edge excitation energies of second period elements with the B3LYP²³ functional,²⁴ albeit via employing spin-contaminated Slater determinants intermediate between singlet and triplet. More recently, some of us have utilized the spin-pure restricted open-shell Kohn-Sham (ROKS) method^{25,26} to predict core-level absorption energies of closed-shell molecules,²⁷ and found ~ 0.2 eV root mean squared error (RMSE) with the SCAN functional.²⁸ Similar performance has also been recently reported for heavier elements²⁹ through the use of the X2C relativistic Hamiltonian.³⁰ OO-DFT methods like ROKS therefore represent an efficient and reliable route for computing core-level absorption spectra.

Nonetheless, the OO-DFT methods have some well-known drawbacks in comparison to TDDFT. It was historically difficult to converge core-excited states without the solver instead collapsing back down to the ground state.²² Recent advances in excited state orbital optimization however offer many routes to avoiding this ‘variational collapse’ problem,^{22,31-37} including the square gradient minimization (SGM) method reported by some of us.³³ In addition, the state specificity of such methods mean that either prior knowledge is necessary to identify desired states or a large number of candidate states have to be individually optimized, making the process considerably more computationally demanding *despite* favorable scaling with system size.¹⁵ In particular, many iterations are often spent trying to converge energies to 10^{-6} hartrees or lower, which seems quite redundant for core-excitations where

uncertainties on the scale of 10^{-3} hartrees (0.03 eV) are unlikely to make an enormous difference as experimental uncertainties are typically of the ~ 0.1 eV scale. However, this does not mean that looser convergence thresholds should be routinely employed for core-level calculations, as it would compromise the precise reproducibility of results (while preserving qualitative agreement) and likely lower the quality of other excited state properties like oscillator strengths or forces.

It is therefore desirable to have protocols that can predict core-excitation energies and properties in a well-defined, reproducible manner, *without* too many excited state specific iterations. There are hybrid schemes that combine OO core-hole relaxation with LR excited state computations, with the best known example being static exchange (STEX).^{38,39} The STEX approach converges core-ionized states with Δ SCF/HF, and then performs configuration interaction singles⁴⁰ (CIS) with the resulting orbitals. Finally, any contribution from the RHF ground state in the final wavefunction removed via projection, although this last contribution is generally quite small as the two states are quite different in character. Ignoring this projection correction, STEX can thus be seen as electron-addition CIS (EA-CIS) atop a core-ionized reference, and is thus LR based (CIS being equivalent to TDHF within the Tamm-Dancoff approximation⁴¹). STEX was subsequently generalized to nonorthogonal CIS^{13,42,43} (NOCIS) for systems with multiple symmetry equivalent atoms. However, use of HF leads to ~ 1.4 eV overestimation in core-level excitation energies of closed-shell molecules with STEX/NOCIS (as can be seen from Table 1), especially for core \rightarrow valence excitations (the errors being generally lower for core \rightarrow Rydberg processes). This is perceptibly greater than the ~ 0.6 eV error with fully OO ROKS/HF.¹⁵ This difference also leads to an impression that STEX spectrum are sometimes ‘compressed’ relative to experiment,¹⁶ as the low lying states with larger valence character are blueshifted much more than the higher energy Rydberg states.

The difference between STEX and ROKS/HF can be interpreted to arise from ROKS/HF fully optimizing the density in the presence of both the particle and the hole, while STEX

only optimizes the density in the presence of the hole and then determines the effect of the particle via CIS. The latter is equivalent to CIS estimating the particle level through a linear combination of virtual orbitals of the core-ionized state. This can be mathematically demonstrated as follows. Let the ROHF determinant for the core ionized state be $|\Phi_+\rangle$, the core-hole orbital be h and $\{a, b, c \dots\}$ the unoccupied orbitals (with there being V such orbitals). Let us further define $|\Phi'\rangle = a_h^\dagger |\Phi_+\rangle$ as the neutral, RHF, core-hole filled state with ROHF core-ionized orbitals. CIS for singlet states therefore involves diagonalization of the Hamiltonian within the subspace spanned by $|\Phi_h^a\rangle = \frac{1}{\sqrt{2}} (a_a^\dagger a_h + a_a^\dagger a_{\bar{h}}) |\Phi'\rangle$, $|\Phi_h^b\rangle = \frac{1}{\sqrt{2}} (a_b^\dagger a_h + a_b^\dagger a_{\bar{h}}) |\Phi'\rangle$ etc. The matrix representation of the Hamiltonian within this V dimensional subspace of singly excited singlet states is given by:

$$A_{ab} = E' \delta_{ab} + F'_{ab} - F'_{hh} \delta_{ab} + 2 \langle hh|ab\rangle - \langle ha|hb\rangle \quad (1)$$

where the Fock operator F' is constructed from $|\Phi'\rangle$ (and not $|\Phi_+\rangle$), while E' is the energy of $|\Phi'\rangle$. If we solve the $\mathbf{AX} = E\mathbf{X}$ CIS eigenproblem, the eigenstates are given by:

$$|\Phi_h^p\rangle = \frac{1}{\sqrt{2}} \sum_a X_{pa} (a_a^\dagger a_h + a_a^\dagger a_{\bar{h}}) |\Phi'\rangle = (a_p^\dagger a_h + a_p^\dagger a_{\bar{h}}) |\Phi'\rangle \quad (2)$$

$$a_p^\dagger = \sum_a X_{pa} a_a^\dagger \quad (3)$$

The final result is therefore a $h \rightarrow p$ excitation from $|\Phi'\rangle$, with the particle level p being a linear combination of the original unoccupied levels $\{a\}$ that is obtained via the CIS procedure through Eq. 3. This connection implies that each unprojected STEEX eigenstate has the form of a spin-adapted open-shell HF wavefunction, analogous to ROKS. However, the hole orbital h and other doubly occupied levels are found via optimization of the core-ionized state $|\Phi_+\rangle$, in contrast to the fully OO ROKS/HF approach that is specific to each excited singlet state.

STEEX's use of an unoptimized, CIS particle level atop core-ionized orbitals instead of a

fully optimized ROKS/HF density should lead to an overestimation of excitation energies, at least for the lowest energy core-excited states. This appears to suggest that a state-specific DFT approach that utilizes the spin-adapted STEX wavefunction $|\Phi_h^p\rangle$ would need to take advantage of some error cancellation in order to have low error. In particular, several generalized gradient approximations (GGAs) like PBE⁴⁴ and B97-D⁴⁵ systematically underestimate core-ionization energies by ~ 1 eV with Δ SCF, suggesting that their use in STEX like protocols can lead to low net error via cancellation of the functional specific underestimation for core-hole formation with the overestimation arising from use of CIS particle levels. The error cancellation in such models can be compared to the manner in which hybrid functionals attempt to mitigate the delocalization error in local KS approaches with the overlocalizing tendency of HF.^{5,23} Such a protocol also has computational advantages, as the OO procedure is necessary only for ionizing every relevant core orbital h , instead of having to independently optimize a particle-hole pair for each excited state with ROKS. In addition, use of pure GGAs avoids the computational burden of computing exact exchange (aside from the single construction of \mathbf{A} per site).

We therefore propose a scheme for computing core-level excitation energies using electronic configurations generated via a STEX like protocol, but using the state-specific ROKS energy ansatz. This requires identification of the particle and hole levels corresponding to the excitation, which we determine as follows:

1. Converge restricted KS equations for the ground state to obtain energy E_0 .
2. Converge the RO core-ionized state with the same functional.
3. Perform CIS atop $|\Phi'\rangle$ generated from the core-ionized RO orbitals and find the particle levels via Eq. 3. Note that this step explicitly uses HF, irrespective of the KS functional used in the preceding steps (i.e. F' etc are found from HF, acting upon KS orbitals).
4. For a given particle level p obtained in the previous step, find the excited state singlet ROKS energy E_S . Let E_M be the KS energy of the spin-contaminated determinant

$a_p^\dagger a_i |\Phi'\rangle$ and E_T the energy of the pure triplet $a_p^\dagger a_{\bar{i}} |\Phi'\rangle$. The determinant $a_p^\dagger a_i |\Phi'\rangle$ is half-singlet and half-triplet,^{25,46} and so $E_S = 2E_M - E_T$.

5. The excitation energy is then $E_S - E_0$.

The use of HF in step 3 irrespective of the chosen KS functional is intentional, in order to have a wavefunction theory based definition of the particle level and to avoid use of KS eigenvalues anywhere in the problem. The use of HF also allows for direct inclusion of relevant double excitations in open-shell systems via XCIS⁴⁷ and related methods,^{42,43} which would be less straightforward with a KS treatment. We also note that the eigenvalues of \mathbf{A} (i.e. CIS state energies) are discarded. The only purpose of CIS is to generate a particle level which can be used to obtain ROKS energies. The method can therefore be described as semi-OO, wherein the doubly occupied levels and the core-hole are identical to the fully optimized core-ionized state while the particle level is found from CIS. We subsequently refer to this hybrid method as ROKS(STEX), as opposed to fully orbital optimized ROKS which is simply referred to as ROKS. We note that ROKS(STEX) with HF would be identical to STEX, if the ground state contribution was not projected out in the latter. It can therefore be viewed as a KS based generalization of STEX, as well as an approximation to the usual ROKS protocol.

It is worthwhile examining the performance of this ROKS(STEX) approach against experiment to determine viability. Table 1 reports performance with a number of GGA functionals (along with the SCAN meta-GGA and the PBE0⁶⁵ hybrid GGA) for the lowest dipole allowed excitation in 40 small molecules. The dataset is dominated by $1s \rightarrow \pi^*$ transitions, which are amongst the hardest to model with STEX. Fully orbital optimized ROKS/SCAN values are supplied, for comparison.

It is immediately apparent that the ROKS(STEX) approaches are nowhere close in accuracy to full OO ROKS/SCAN, which has a quite low RMSE of 0.2 eV and virtually no systematic bias. On the other hand, ROKS(STEX)/SCAN overestimates energies by ~ 1 eV due to the suboptimal nature of the CIS derived particle orbital as compared to

Table 1: Lowest dipole allowed K-edge excitation energies (in eV) for 40 small molecules, at the C,N,O,F K-edges. The site of the excitation is bolded (or otherwise specified within parentheses). Root mean squared error (RMSE), mean signed error (ME), maximum absolute error (MAX) and mean absolute error (MAE) vs experiment are also reported. Further details about calculations are reported in the computational methods section.

Species	Expt	SCAN (OO)	SCAN	PBE	PBE0	B88 ⁴⁸	OLYP ^{49,50}	B97-D	STEX
C ₂ H ₄	284.7 ⁵¹	284.7	285.8	285.0	285.4	285.3	285.2	285.3	286.4
H CHO	285.6 ⁵²	285.8	287.4	286.5	286.8	286.9	286.6	286.6	288.2
C ₂ H ₂	285.9 ⁵¹	285.7	286.5	285.6	286.0	285.9	285.8	285.9	287.3
C ₂ N ₂	286.3 ⁵³	286.3	287.3	286.3	286.7	286.7	286.4	286.5	288.3
H CN	286.4 ⁵³	286.4	287.5	286.6	286.9	286.9	286.7	286.7	288.2
Me ₂ C O	286.4 ⁵⁴	286.5	288.2	287.3	287.7	287.7	287.4	287.3	289.2
C ₂ H ₆	286.9 ⁵¹	286.8	287.2	286.2	286.6	286.0	286.5	286.8	287.5
C O	287.4 ⁵⁵	287.1	288.2	287.3	287.7	287.6	287.3	287.4	289.2
C H ₄	288.0 ⁵⁶	288.0	288.2	287.1	287.6	286.9	287.4	287.5	288.5
CH ₃ O H	288.0 ⁵⁴	288.2	288.6	287.5	288.0	287.4	287.8	288.2	289.1
H COOH	288.1 ⁵⁴	288.0	289.5	288.5	288.9	288.9	288.6	288.6	290.5
H COF	288.2 ⁵⁷	288.2	289.7	288.7	289.1	289.1	288.8	288.8	290.8
C O ₂	290.8 ⁵⁸	290.4	291.5	290.3	290.9	290.8	290.4	290.4	293.1
CF ₂ O	290.9 ⁵⁷	290.6	292.1	291.0	291.6	291.5	291.1	291.2	293.6
C ₂ N ₂	398.9 ⁵³	398.9	399.7	398.8	399.1	399.2	398.8	398.6	400.4
H CN	399.7 ⁵³	399.7	400.5	399.6	399.9	399.9	399.6	399.5	401.0
Imidazole (N)	399.9 ⁵⁹	399.9	400.9	400.0	400.4	400.2	400.0	399.9	401.3
N H ₃	400.8 ⁵⁶	400.5	401.0	399.9	400.3	399.8	400.1	400.2	401.2
N ₂	400.9 ⁶⁰	400.9	402.1	401.2	401.5	401.5	401.1	400.9	402.6
N NO	401.0 ⁵⁸	401.1	402.4	401.4	401.7	401.8	401.4	401.2	402.8
Glycine (N)	401.2 ⁶¹	401.1	401.7	400.7	401.1	400.4	400.8	400.9	402.0
Pyrrole (N)	402.3 ⁶²	402.3	403.0	402.0	402.4	401.6	402.1	401.9	402.9
Imidazole (NH)	402.3 ⁵⁹	402.4	403.1	402.2	402.6	401.9	402.2	402.1	403.3
N NO	404.6 ⁵⁸	404.5	405.7	404.7	405.1	405.0	404.5	404.4	406.6
H CHO	530.8 ⁵²	530.9	532.1	531.3	531.4	531.6	531.0	530.7	531.9
Me ₂ C O	531.4 ⁵⁴	531.3	532.7	531.8	531.9	532.2	531.5	531.1	532.8
H COF	532.1 ⁵⁷	532.1	533.3	532.4	532.5	532.7	532.2	531.8	533.2
H COOH (O)	532.2 ⁵⁴	532.0	533.2	532.3	532.4	532.6	532.0	531.6	533.1
CF ₂ O	532.7 ⁵⁷	533.1	534.4	533.5	533.6	533.9	533.3	532.8	534.4
H ₂ O	534.0 ⁵⁶	533.9	534.4	533.2	533.6	533.2	533.2	533.0	534.5
CH ₃ O H	534.1 ⁵⁴	534.0	534.7	533.6	533.9	533.4	533.5	533.3	534.5
C O	534.2 ⁵⁵	534.2	535.2	534.3	534.4	534.5	534.0	533.6	534.9
N NO	534.6 ⁵⁸	535.1	536.3	535.4	535.3	535.7	535.2	534.8	535.7
Furan (O)	535.2 ⁶³	535.2	535.9	534.9	535.2	535.1	534.8	534.3	536.0
H COOH (OH)	535.4 ⁵⁴	535.5	536.5	535.5	535.8	535.8	535.4	535.0	536.5
C O ₂	535.4 ⁵⁸	535.6	536.6	535.5	535.7	535.9	535.3	534.9	536.7
F ₂	682.2 ⁶⁴	682.5	685.3	684.4	684.3	685.0	683.8	683.1	684.3
H F	687.4 ⁶⁴	687.5	688.0	686.7	687.0	686.8	686.4	686.0	687.7
H COF	687.7 ⁵⁷	688.0	688.9	687.8	688.0	688.2	687.4	686.9	689.0
CF ₂ O	689.2 ⁵⁷	689.6	690.8	689.6	689.8	690.0	689.2	688.6	690.8
RMSE		0.20	1.18	0.58	0.62	0.82	0.51	0.55	1.56
ME		0.01	1.05	0.06	0.37	0.29	0.01	-0.14	1.40
MAX		0.49	3.09	2.21	2.07	2.83	1.60	1.39	2.76

full orbital relaxation. SCAN predicts quite accurate Δ SCF core-electron binding energies,^{27,66,67} and therefore the error arising from the unrelaxed particle level remains uncancelled. ROKS(STEX)/SCAN is nonetheless a perceptible improvement over standard STEX, which overestimates by 1.4 eV. It is nonetheless worth noting that STEX has a lower error for F_2 than ROKS(STEX)/SCAN, resulting in a smaller maximum absolute error.

However, use of functionals that systematically underestimate core-level excitation energies with ROKS can lead to lower error with ROKS(STEX). This is quite visible for the GGAs OLYP, PBE and B97-D (with the full ROKS numbers being provided in the supporting information). These three GGAs have a reasonably low ROKS(STEX) RMSE of 0.5-0.6 eV, which is nonetheless $3\times$ larger than what can be obtained from ROKS/SCAN. Perhaps more importantly, the maximum error for all three exceeds 1 eV (while ROKS/SCAN only has 0.5 eV maximum deviation from experiment), with F_2 and the C K-edge of HCHO being particularly challenging cases where ROKS(STEX) continues to greatly overestimate.

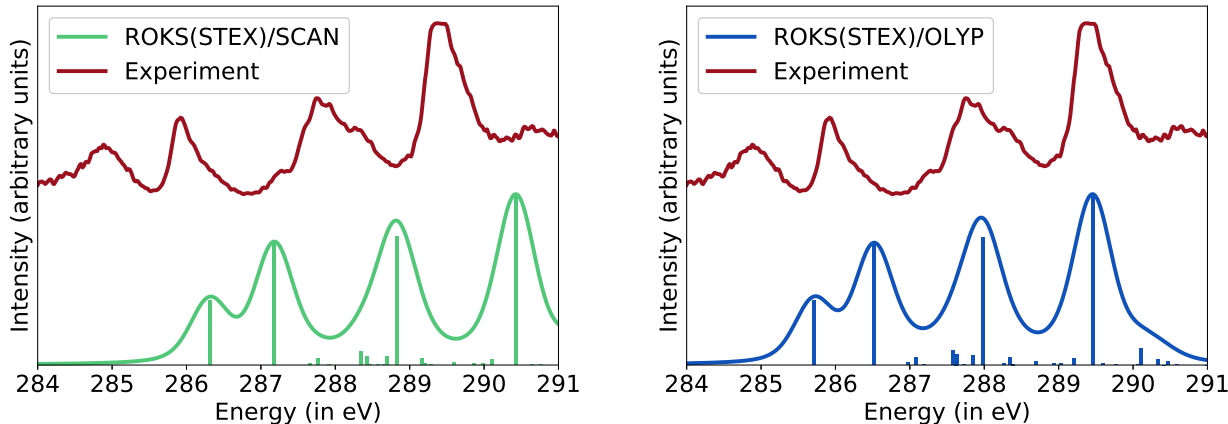


Figure 1: C K-edge XAS of thymine computed from ROKS(STEX) with SCAN (left) and OLYP (right) as compared to experiment.⁶⁸ The computed peaks were broadened by a Voigt profile with a Gaussian $\sigma = 0.2$ eV and Lorentzian $\gamma = 0.121$ eV.

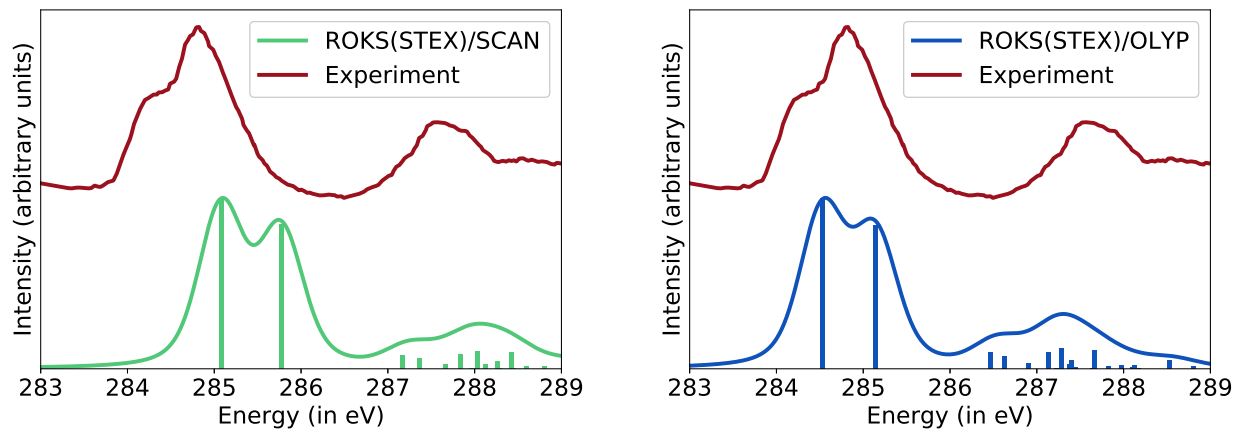
We next consider the quality of the complete spectrum predicted by ROKS(STEX). Fig. 1 presents the experimental C K-edge of thymine⁶⁸ vs ROKS(STEX) results from SCAN and OLYP. It can be seen that the general shape of the spectrum is reproduced well, although the peak positions are quite suboptimal. The peaks computed with SCAN are ~ 1 eV

over experimental results, and reasonable agreement can be found if the computed spectrum is redshifted by 1 eV. On the other hand, the OLYP spectrum is quite compressed, with agreement for the two highest energy peaks being quite adequate, while the lowest energy peak is overestimated by ~ 0.7 eV. The compression of the spectrum here is particularly interesting, since all the peaks arise from $1s \rightarrow \pi^*$ transitions. Nonetheless, this behavior is consistent with the results reported in Table 1, where OLYP overestimated the C K-edge $1s \rightarrow \pi^*$ excitation of HCHO by 1 eV, while being essentially spot on for CO. The ROKS(STEX) excitation energies are therefore nowhere as accurate as full ROKS with OO, leading to deleterious consequences for the overall spectrum.

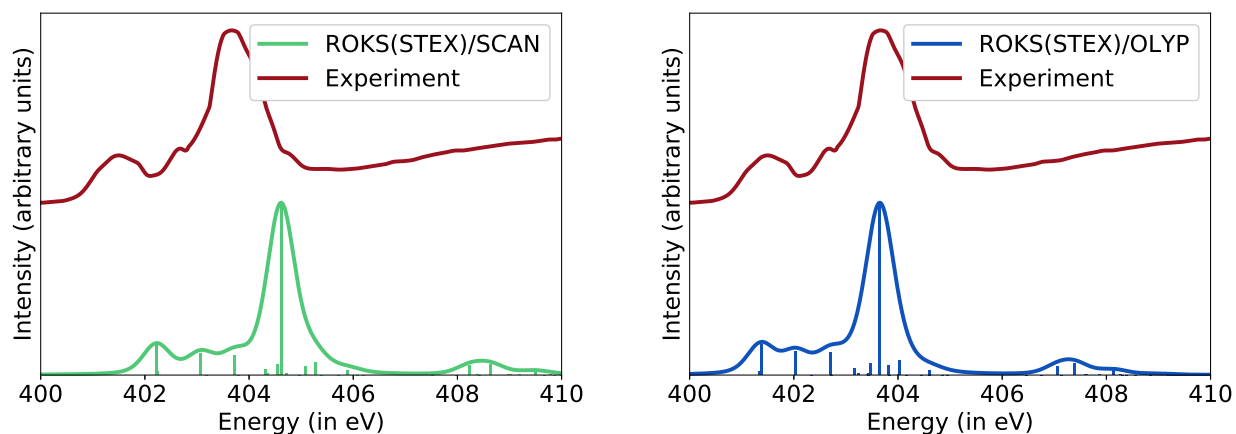
On a more optimistic note, oscillator strengths from the ROKS(STEX) approach seem to be adequately accurate. It is thus possible to envision a procedure in which ROKS(STEX) is used to identify the *significant* contributors to the absorption spectrum, followed by full OO on these states to have a more accurate result. Such a protocol thus be effective in reducing computational cost by screening out many weakly absorbing Rydberg type excitations for which full OO is not necessary and ROKS(STEX) energies/oscillator strengths are adequate.

It therefore appears that there are two possible routes to utilize the ROKS(STEX) approach. The first is to use it exclusively for computing spectra with a GGA like OLYP or B97-D, relying on the cancellation of errors between the core-ionization energy underestimation by these functionals and the overestimation from use of the unoptimized STEX particle level. This approach is considerably more computationally efficient than ROKS/SCAN, both because it is core-orbital (site) specific as opposed to state specific, and because it only employs a GGA. The errors nonetheless would be much larger, and the prediction quality can be compromised such as in the case of thymine shown in Fig 1. On the other hand, reasonable results are also possible at times, such as in the case of butadiene, 4-nitroaniline, and 4-hydroxybenzoic acid (as shown in Fig 2).

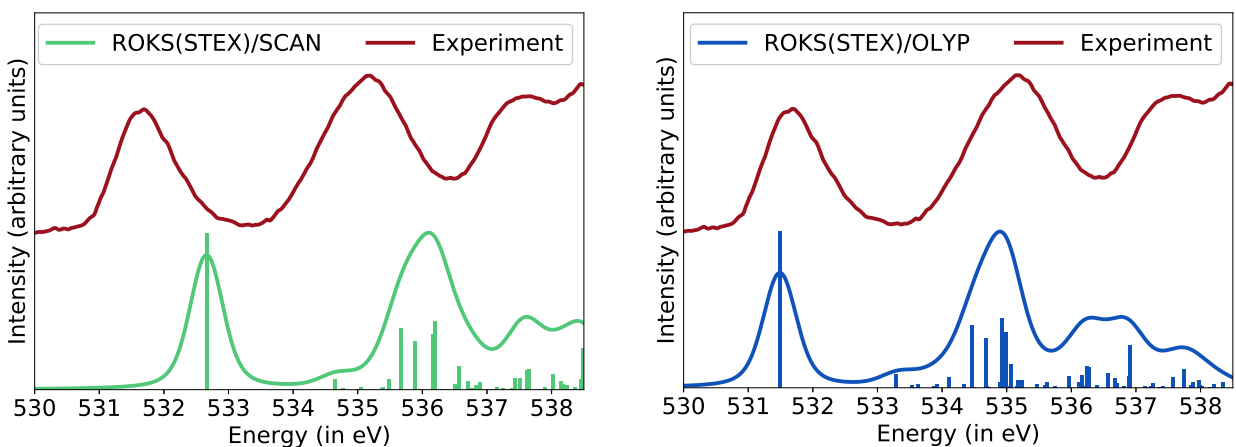
The second way to use ROKS(STEX) is in conjunction with full ROKS. ROKS(STEX) with SCAN can be first used to get an approximate sense of how the spectrum will look, and



(a) C K-edge XAS of 1,3-butadiene.⁶⁹



(b) N K-edge XAS of 4-nitroaniline.⁷⁰



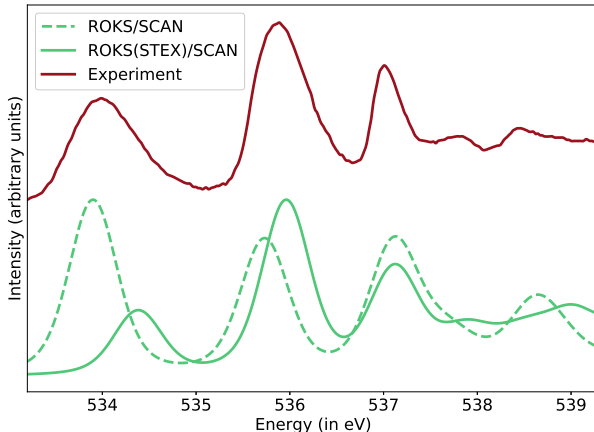
(c) O K-edge XAS of 4-hydroxybenzoic acid.⁷¹

Figure 2: ROKS(STEX) spectra compared to experiment. Computed peaks were broadened by a Voigt profile with a Gaussian $\sigma = 0.2$ eV and Lorentzian $\gamma = 0.121$ eV.

Table 2: O K-edge excitations of H₂O, via SCAN. Other than the first two states (which are of mixed valence-Rydberg character) the rest are almost purely Rydberg.

State	ROKS	ROKS(STEX)	Symmetry
1	533.90	534.38	A ₁
2	535.73	535.96	B ₂
3	537.04	537.07	B ₁
4	537.14	537.20	A ₁
5	537.58	537.72	A ₁
6	537.82	537.95	B ₂
7	538.24	538.26	A ₁
8	538.25	538.28	A ₂
9	538.36	538.38	B ₂
10	538.47	538.51	B ₁

(a) Excitation energies



(b) Computed XAS compared to experiment.⁵⁶

identify the transitions with large oscillator strengths that are below the ionization threshold. These transitions can then be specifically optimized using ROKS, in order to obtain more accurate energies. The remaining low intensity transitions can be left at the ROKS(STEX) level as they will have a rather low effect on the full near edge spectrum. These transitions furthermore will likely contain a large number of Rydberg states, which should be reasonably predicted by the ROKS(STEX) approach since the particle-hole interaction in such cases will be weak enough to make EA-CIS an acceptable approximation. As evidence, we list the core-excited states of H₂O and compare the full OO ROKS results with ROKS(STEX) in Table 2a. It is clear that the Rydberg states predicted by ROKS(STEX) are within 0.1 eV of the full ROKS optimized state, indicating ROKS(STEX)'s efficacy in efficiently modeling such states. Indeed, the ROKS(STEX) spectrum is very similar in quality to the ROKS spectrum for H₂O, as shown in Table 2.

In conclusion, ROKS(STEX) is a site-specific, computationally efficient method for accessing the core-level spectra of closed-shell molecules. It employs particle levels obtained via EA-CIS atop a core-ionized state, and is therefore less accurate than a fully orbital optimized method like ROKS (with a good functional like SCAN). Nonetheless, cancellation of errors can be carefully employed to have ROKS(STEX) yield results with low systematic error

and reasonably low RMSE with GGA functionals like OLYP or B97-D. ROKS(STEX) can also be used to screen excitations a-priori to determine which ones have significant oscillator strengths. These strong intensity transitions can then be accessed via ROKS proper, while the remaining weakly absorbing states are left at the ROKS(STEX) level.

In future, we intend to investigate the utility of this approach for open-shell systems, where CIS has to be extended to include some double (or higher order) excitations in order to obtain spin-pure results.⁴⁷ This can prove useful in interpreting XAS spectra collected to study photochemical dynamics of large systems, as it would assist in decoupling the critical valence excitations that require full OO treatment from the many Rydberg levels that are adequately treated with STEX like approaches.

Computational methods

All calculations were performed with a development version of the Q-Chem 5.4 package.⁷² Local exchange–correlation integrals for DFT were calculated over a radial grid with 99 points and an angular Lebedev grid with 590 points. The spin-free one-electron X2C relativistic Hamiltonian was used for all calculations.^{29,30} For nearly all calculations, the site of the core excitation used an aug-pcX-2 basis,⁷³ while aug-pcseg-1⁷⁴ was used for all other atoms. A mixed basis strategy of this nature was previously found to be practically equivalent to purely using the larger basis, for core-level excitation energies.²⁷ This also served to localize the core-hole onto a single atom for species with equivalent atoms (like O in CO₂), and thus prevented errors arising from delocalization^{4,5} of the hole over multiple sites.²⁷ The one exception regarding basis sets is the data for Table 2, for which the doubly augmented d-aug-pc-2 basis was used instead. The geometries utilized were obtained from Ref 27. They are also provided in the supporting information, for convenience.

Acknowledgment

This work was supported by the Director, Office of Science, Office of Basic Energy Sciences, of the U.S. Department of Energy under Contract No. DE-AC02-05CH11231, through the Atomic, Molecular, and Optical Sciences Program of the Chemical Sciences Division of Lawrence Berkeley National Laboratory. Additional support came from the Liquid Sunlight Alliance, which is funded by the U.S. Department of Energy, Office of Science, Office of Basic Energy Sciences, Fuels from Sunlight Hub under Award Number DE-SC0021266.

Data Availability

The data that supports the findings of this study are available within the article and its supplementary material.

Supporting Information

XLXS: Raw data.

ZIP: Geometries of all species considered in xyz format.

Conflicts of Interest

M.H.-G. is a part-owner of Q-Chem, which is the software platform in which the developments described here were implemented.

References

- (1) Casida, M. E. Time-dependent density functional response theory for molecules. In *Recent Advances In Density Functional Methods: (Part I)*; World Scientific, 1995; pp 155–192.

- (2) Dreuw, A.; Head-Gordon, M. Single-reference ab initio methods for the calculation of excited states of large molecules. *Chem. Rev.* **2005**, *105*, 4009–4037.
- (3) Runge, E.; Gross, E. K. U. Density-functional theory for time-dependent systems. *Phys. Rev. Lett.* **1984**, *52*, 997.
- (4) Perdew, J. P.; Parr, R. G.; Levy, M.; Balduz Jr, J. L. Density-functional theory for fractional particle number: derivative discontinuities of the energy. *Phys. Rev. Lett.* **1982**, *49*, 1691.
- (5) Hait, D.; Head-Gordon, M. Delocalization errors in density functional theory are essentially quadratic in fractional occupation number. *J. Phys. Chem. Lett.* **2018**, *9*, 6280–6288.
- (6) Dreuw, A.; Weisman, J. L.; Head-Gordon, M. Long-range charge-transfer excited states in time-dependent density functional theory require non-local exchange. *J. Chem. Phys.* **2003**, *119*, 2943–2946.
- (7) Dreuw, A.; Head-Gordon, M. Failure of time-dependent density functional theory for long-range charge-transfer excited states: the zincbacteriochlorin- bacteriochlorin and bacteriochlorophyll- spheroidene complexes. *J. Am. Chem. Soc.* **2004**, *126*, 4007–4016.
- (8) Maitra, N. T.; Zhang, F.; Cave, R. J.; Burke, K. Double excitations within time-dependent density functional theory linear response. *J. Chem. Phys.* **2004**, *120*, 5932–5937.
- (9) Li, Z.; Liu, W. Critical Assessment of TD-DFT for Excited States of Open-Shell Systems: I. Doublet–Doublet Transitions. *J. Chem. Theory Comput.* **2016**, *12*, 238–260.
- (10) Hait, D.; Haugen, E. A.; Yang, Z.; Oosterbaan, K. J.; Leone, S. R.; Head-Gordon, M. Accurate prediction of core-level spectra of radicals at density functional theory cost via

- square gradient minimization and recoupling of mixed configurations. *J. Chem. Phys.* **2020**, *153*, 134108.
- (11) Hait, D.; Rettig, A.; Head-Gordon, M. Beyond the Coulson–Fischer point: characterizing single excitation CI and TDDFT for excited states in single bond dissociations. *Phys. Chem. Chem. Phys.* **2019**, *21*, 21761–21775.
- (12) Besley, N. A.; Asmuruf, F. A. Time-dependent density functional theory calculations of the spectroscopy of core electrons. *Phys. Chem. Chem. Phys.* **2010**, *12*, 12024–12039.
- (13) Oosterbaan, K. J.; White, A. F.; Head-Gordon, M. Non-orthogonal configuration interaction with single substitutions for the calculation of core-excited states. *J. Chem. Phys.* **2018**, *149*, 044116.
- (14) Besley, N. A.; Peach, M. J.; Tozer, D. J. Time-dependent density functional theory calculations of near-edge X-ray absorption fine structure with short-range corrected functionals. *Phys. Chem. Chem. Phys.* **2009**, *11*, 10350–10358.
- (15) Hait, D.; Head-Gordon, M. Orbital optimized density functional theory for electronic excited states. *J. Phys. Chem. Lett.* **2021**, *12*, 4517–4529.
- (16) Norman, P.; Dreuw, A. Simulating X-ray spectroscopies and calculating core-excited states of molecules. *Chemical reviews* **2018**, *118*, 7208–7248.
- (17) Vidal, M. L.; Feng, X.; Epifanovsky, E.; Krylov, A. I.; Coriani, S. New and efficient equation-of-motion coupled-cluster framework for core-excited and core-ionized states. *J. Chem. Theory Comput.* **2019**, *15*, 3117–3133.
- (18) Carbone, J. P.; Cheng, L.; Myhre, R. H.; Matthews, D.; Koch, H.; Coriani, S. An analysis of the performance of coupled cluster methods for K-edge core excitations and ionizations using standard basis sets. In *Adv. Quantum Chem.*; Elsevier, 2019; Vol. 79; pp 241–261.

- (19) Wenzel, J.; Wormit, M.; Dreuw, A. Calculating core-level excitations and x-ray absorption spectra of medium-sized closed-shell molecules with the algebraic-diagrammatic construction scheme for the polarization propagator. *J. Comput. Chem.* **2014**, *35*, 1900–1915.
- (20) Kraus, P. M.; Zürich, M.; Cushing, S. K.; Neumark, D. M.; Leone, S. R. The ultrafast X-ray spectroscopic revolution in chemical dynamics. *Nat. Rev. Chem.* **2018**, *2*, 82–94.
- (21) Geneaux, R.; Marroux, H. J.; Guggenmos, A.; Neumark, D. M.; Leone, S. R. Transient absorption spectroscopy using high harmonic generation: a review of ultrafast X-ray dynamics in molecules and solids. *Phil. Trans. Roy. Soc. A* **2019**, *377*, 20170463.
- (22) Gilbert, A. T.; Besley, N. A.; Gill, P. M. W. Self-consistent field calculations of excited states using the maximum overlap method (MOM). *J. Phys. Chem. A* **2008**, *112*, 13164–13171.
- (23) Becke, A. D. Density-functional thermochemistry. III. The role of exact exchange. *J. Chem. Phys.* **1993**, *98*, 5648–5652.
- (24) Besley, N. A.; Gilbert, A. T.; Gill, P. M. W. Self-consistent-field calculations of core excited states. *J. Chem. Phys.* **2009**, *130*, 124308.
- (25) Frank, I.; Hutter, J.; Marx, D.; Parrinello, M. Molecular dynamics in low-spin excited states. *J. Chem. Phys.* **1998**, *108*, 4060–4069.
- (26) Kowalczyk, T.; Tsuchimochi, T.; Chen, P.-T.; Top, L.; Van Voorhis, T. Excitation energies and Stokes shifts from a restricted open-shell Kohn-Sham approach. *J. Chem. Phys.* **2013**, *138*, 164101.
- (27) Hait, D.; Head-Gordon, M. Highly Accurate Prediction of Core Spectra of Molecules at Density Functional Theory Cost: Attaining Sub-electronvolt Error from a Restricted Open-Shell Kohn-Sham Approach. *J. Phys. Chem. Lett.* **2020**, *11*, 775–786.

- (28) Sun, J.; Ruzsinszky, A.; Perdew, J. P. Strongly Constrained and Appropriately Normed Semilocal Density Functional. *Phys. Rev. Lett.* **2015**, *115*, 036402.
- (29) Cunha, L. A.; Hait, D.; Kang, R.; Mao, Y.; Head-Gordon, M. Relativistic Orbital Optimized Density Functional Theory for Accurate Core-Level Spectroscopy. *arXiv preprint arXiv:2111.08405* **2021**,
- (30) Saue, T. Relativistic Hamiltonians for Chemistry: A Primer. *Chem. Phys. Chem.* **2011**, *12*, 3077–3094.
- (31) Barca, G. M.; Gilbert, A. T.; Gill, P. M. W. Simple Models for Difficult Electronic Excitations. *J. Chem. Theory Comput.* **2018**, *14*, 1501–1509.
- (32) Shea, J. A.; Gwin, E.; Neuscanner, E. A generalized variational principle with applications to excited state mean field theory. *J. Chem. Theory Comput.* **2020**, *16*, 1526–1540.
- (33) Hait, D.; Head-Gordon, M. Excited state orbital optimization via minimizing the square of the gradient: General approach and application to singly and doubly excited states via density functional theory. *J. Chem. Theory Comput.* **2020**, *16*, 1699–1710.
- (34) Carter-Fenk, K.; Herbert, J. M. State-Targeted Energy Projection: A Simple and Robust Approach to Orbital Relaxation of Non-Aufbau Self-Consistent Field Solutions. *J. Chem. Theory Comput.* **2020**, *16*, 5067–5082.
- (35) Levi, G.; Ivanov, A. V.; Jónsson, H. Variational density functional calculations of excited states via direct optimization. *J. Chem. Theory Comput.* **2020**, *16*, 6968–6982.
- (36) Ye, H.-Z.; Welborn, M.; Ricke, N. D.; Van Voorhis, T. σ -SCF: A direct energy-targeting method to mean-field excited states. *J. Chem. Phys.* **2017**, *147*, 214104.
- (37) Corzo, H. H.; Abou Taka, A.; Pribram-Jones, A.; Hratchian, H. P. Using projection

- operators with maximum overlap methods to simplify challenging self-consistent field optimization. *J. Comp. Chem.* **2022**, *43*, 382–390.
- (38) Ågren, H.; Carravetta, V.; Vahtras, O.; Pettersson, L. G. Direct, atomic orbital, static exchange calculations of photoabsorption spectra of large molecules and clusters. *Chemical physics letters* **1994**, *222*, 75–81.
- (39) Ågren, H.; Carravetta, V.; Vahtras, O.; Pettersson, L. G. Direct SCF direct static-exchange calculations of electronic spectra. *Theo. Chem. Acc.* **1997**, *97*, 14–40.
- (40) Foresman, J. B.; Head-Gordon, M.; Pople, J. A.; Frisch, M. J. Toward a systematic molecular orbital theory for excited states. *J. Phys. Chem.* **1992**, *96*, 135–149.
- (41) Hirata, S.; Head-Gordon, M. Time-dependent density functional theory within the Tamm–Dancoff approximation. *Chem. Phys. Lett.* **1999**, *314*, 291–299.
- (42) Oosterbaan, K. J.; White, A. F.; Head-Gordon, M. Non-orthogonal configuration interaction with single substitutions for core-excited states: An extension to doublet radicals. *J. Chem. Theory Comput.* **2019**, *15*, 2966–2973.
- (43) Oosterbaan, K. J.; White, A. F.; Hait, D.; Head-Gordon, M. Generalized single excitation configuration interaction: an investigation into the impact of the inclusion of non-orthogonality on the calculation of core-excited states. *Phys. Chem. Chem. Phys.* **2020**, *22*, 8182–8192.
- (44) Perdew, J. P.; Burke, K.; Ernzerhof, M. Generalized gradient approximation made simple. *Phys. Rev. Lett.* **1996**, *77*, 3865.
- (45) Grimme, S. Semiempirical GGA-type density functional constructed with a long-range dispersion correction. *J. Comput. Chem.* **2006**, *27*, 1787–1799.
- (46) Ziegler, T.; Rauk, A.; Baerends, E. J. On the calculation of multiplet energies by the Hartree-Fock-Slater method. *Theor. Chim. Acta.* **1977**, *43*, 261–271.

- (47) Maurice, D.; Head-Gordon, M. On the nature of electronic transitions in radicals: An extended single excitation configuration interaction method. *J. Phys. Chem.* **1996**, *100*, 6131–6137.
- (48) Becke, A. D. Density-functional exchange-energy approximation with correct asymptotic behavior. *Phys. Rev. A* **1988**, *38*, 3098.
- (49) Handy, N. C.; Cohen, A. J. Left-right correlation energy. *Mol. Phys.* **2001**, *99*, 403–412.
- (50) Lee, C.; Yang, W.; Parr, R. G. Development of the Colle-Salvetti correlation-energy formula into a functional of the electron density. *Phys. Rev. B* **1988**, *37*, 785.
- (51) Hitchcock, A.; Brion, C. Carbon K-shell excitation of C₂H₂, C₂H₄, C₂H₆ and C₆H₆ by 2.5 keV electron impact. *J. Electron Spectrosc. Relat. Phenom.* **1977**, *10*, 317–330.
- (52) Remmers, G.; Domke, M.; Puschmann, A.; Mandel, T.; Xue, C.; Kaindl, G.; Hudson, E.; Shirley, D. High-resolution [ital K]-shell photoabsorption in formaldehyde. *Phys. Rev. A. General Physics;(United States)* **1992**, *46*.
- (53) Hitchcock, A.; Brion, C. Inner shell electron energy loss studies of HCN and C₂N₂. *Chem. Phys.* **1979**, *37*, 319–331.
- (54) Prince, K. C.; Richter, R.; de Simone, M.; Alagia, M.; Coreno, M. Near edge X-ray absorption spectra of some small polyatomic molecules. *J. Phys. Chem. A* **2003**, *107*, 1955–1963.
- (55) Domke, M.; Xue, C.; Puschmann, A.; Mandel, T.; Hudson, E.; Shirley, D.; Kaindl, G. Carbon and oxygen K-edge photoionization of the CO molecule. *Chem. Phys. Lett.* **1990**, *173*, 122–128.
- (56) Schirmer, J.; Trofimov, A.; Randall, K.; Feldhaus, J.; Bradshaw, A.; Ma, Y.; Chen, C.; Sette, F. K-shell excitation of the water, ammonia, and methane molecules using high-resolution photoabsorption spectroscopy. *Phys. Rev. A* **1993**, *47*, 1136.

- (57) Robin, M. B.; Ishii, I.; McLaren, R.; Hitchcock, A. P. Fluorination effects on the inner-shell spectra of unsaturated molecules. *J. Electron Spectrosc. Relat. Phenom.* **1988**, *47*, 53–92.
- (58) Prince, K.; Avaldi, L.; Coreno, M.; Camilloni, R.; De Simone, M. Vibrational structure of core to Rydberg state excitations of carbon dioxide and dinitrogen oxide. *J. Phys. B: At. Mol. Opt. Phys.* **1999**, *32*, 2551.
- (59) Apen, E.; Hitchcock, A. P.; Gland, J. L. Experimental studies of the core excitation of imidazole, 4, 5-dicyanoimidazole, and s-triazine. *J. Phys. Chem* **1993**, *97*, 6859–6866.
- (60) Myhre, R. H.; Wolf, T. J.; Cheng, L.; Nandi, S.; Coriani, S.; Gühr, M.; Koch, H. A theoretical and experimental benchmark study of core-excited states in nitrogen. *J. Chem. Phys.* **2018**, *148*, 064106.
- (61) Plekan, O.; Feyer, V.; Richter, R.; Coreno, M.; De Simone, M.; Prince, K.; Caravatta, V. An X-ray absorption study of glycine, methionine and proline. *J. Electron Spectrosc. Relat. Phenom.* **2007**, *155*, 47–53.
- (62) Pavlychev, A.; Hallmeier, K.; Hennig, C.; Hennig, L.; Szargan, R. Nitrogen K-shell excitations in complex molecules and polypyrrole. *Chem. Phys.* **1995**, *201*, 547–555.
- (63) Dufflot, D.; Flament, J.-P.; Giuliani, A.; Heinesch, J.; Hubin-Franskin, M.-J. Core shell excitation of furan at the O 1s and C 1s edges: An experimental and ab initio study. *J. Chem. Phys.* **2003**, *119*, 8946–8955.
- (64) Hitchcock, A.; Brion, C. K-shell excitation of HF and F₂ studied by electron energy-loss spectroscopy. *J. Phys. B: At. Mol. Phys.* **1981**, *14*, 4399.
- (65) Adamo, C.; Barone, V. Toward reliable density functional methods without adjustable parameters: The PBE0 model. *J. Chem. Phys.* **1999**, *110*, 6158–6170.

- (66) Kahk, J. M.; Lischner, J. Accurate absolute core-electron binding energies of molecules, solids, and surfaces from first-principles calculations. *Phys. Rev. Materials* **2019**, *3*, 100801.
- (67) Kahk, J. M.; Michelitsch, G. S.; Maurer, R. J.; Reuter, K.; Lischner, J. Core Electron Binding Energies in Solids from Periodic All-Electron Δ -Self-Consistent-Field Calculations. *J. Phys. Chem. Lett.* **2021**, *12*, 9353–9359, PMID: 34549969.
- (68) Plekan, O.; Feyer, V.; Richter, R.; Coreno, M.; De Simone, M.; Prince, K.; Trofimov, A.; Gromov, E.; Zaytseva, I.; Schirmer, J. A theoretical and experimental study of the near edge X-ray absorption fine structure (NEXAFS) and X-ray photoelectron spectra (XPS) of nucleobases: Thymine and adenine. *Chem. Phys.* **2008**, *347*, 360–375.
- (69) Sodhi, R. N.; Brion, C. High resolution carbon 1s and valence shell electronic excitation spectra of trans-1, 3-butadiene and allene studied by electron energy loss spectroscopy. *J. Electron Spectrosc. Relat. Phenom.* **1985**, *37*, 1–21.
- (70) Turci, C. C.; Urquhart, S. G.; Hitchcock, A. P. Inner-shell excitation spectroscopy of aniline, nitrobenzene, and nitroanilines. *Can. J. Chem.* **1996**, *74*, 851–869.
- (71) Hill, A.; Sa'adeh, H.; Cameron, D.; Wang, F.; Trofimov, A. B.; Larionova, E. Y.; Richter, R.; Prince, K. C. Positional and Conformational Isomerism in Hydroxybenzoic Acid: A Core-Level Study and Comparison with Phenol and Benzoic Acid. *J. Phys. Chem. A* **2021**, *125*, 9877–9891.
- (72) Epifanovsky, E., et al. Software for the frontiers of quantum chemistry: An overview of developments in the Q-Chem 5 package. *J. Chem. Phys.* **2021**, *155*, 084801.
- (73) Ambrose, M. A.; Jensen, F. Probing Basis Set Requirements for Calculating Core Ionization and Core Excitation Spectroscopy by the Δ Self-Consistent-Field Approach. *J. Chem. Theory Comput.* **2018**, *15*, 325–337.

- (74) Jensen, F. Unifying general and segmented contracted basis sets. Segmented polarization consistent basis sets. *J. Chem. Theory Comput.* **2014**, *10*, 1074–1085.